Adsorption of Ar atoms on the relaxed defect-free TiO$_2$(110) surface

J. R. B. Gomes[1,2] and J. P. Prates Ramalho[3,4]

[1]*Centro de Investigação em Química, Faculdade de Ciências da Universidade do Porto, R. do Campo Alegre 687, P-4169-007 Porto, Portugal*

[2]*Departament de Química-Física i Centre de Recerca en Química Teòrica, Universitat de Barcelona i Parc Científic de Barcelona, C/Martí i Franquès 1, E-08028 Barcelona, Spain*

[3]*Departamento de Química, Universidade de Évora, R. Romão Ramalho, 59, 7000 Évora, Portugal*

[4]*CFTC, Av. Prof. Gama Pinto 2, P-1649-003 Lisboa, Portugal*

The interaction of Ar atoms with the relaxed and defect-free TiO$_2$(110) surface was investigated by means of density functional theory within the GGA/PW91 exchange-correlation functional. A periodic three-dimensional slab plus vacuum width was used to model both the clean and Ar covered rutile surface. The calculations predict an important interlayer relaxation of the clean oxide surface when compared with the bulk rutile structure. The computed interaction energies are very small when atomic argon is deposited above this surface as expected for a physisorbed state. It was found that Ar prefers to interact with low coordination sites as found experimentally and theoretically for rare gases adsorbed on transition metal surfaces. On the rutile surface, Ar adsorbs preferentially on fivefold coordinated Ti sites, with an adsorbate to substrate height similar to that found experimentally for the Ar/Ag(111) system, while the least favorable site for adsorption is atop protruding oxygen atoms. The computed interaction energy on the most favorable adsorption site is 42 meV, almost 1/2 to 1/3 of the experimental binding energies recently reported for Ar adsorption on Ag(111), Ni(111), Pd(111), and Pt(111) surfaces.

I. INTRODUCTION

Rutile titanium dioxide is an important material with a wide range of applications in several areas of material and surface science such as catalysis, photocatalysis, and microelectronics.[1,2] Historically it has been used as catalyst, pigment, opacifier, filler, etc. Recently, this material gained even more attention due to the extraordinarily high activity for low temperature catalytic combustion, partial oxidation of hydrocarbons, hydrogenation of unsaturated hydrocarbons, and reduction of nitrogen oxides catalyzed by ultrafine gold particles dispersed on TiO$_2$.[2] Rutile has a high index of refraction and dispersion and absorbs strongly UV radiation. It is also a large-band gap semiconductor and has a high dielectric constant. Besides the many interesting physical properties it holds, rutile is both an environment friendly and biocompatible material which has been employed in food and pharmaceutical industries.[3] Because of the importance of rutile as an industrial and technological material it has been the focus of intense research in recent years. Although rutile has been so widely studied, both theoretically and experimentally, there is still controversy about the exact structure of its relaxed surface. *Ab initio* techniques such as Hartree-Fock and density functional theory have been used to study the low index rutile crystallographic planes.[4–8] Experimentally, it has been characterized by a large number of techniques including low-energy electron diffraction (LEED),[9] scanning tunneling microscopy (STM),[10–13] surface x-ray diffraction (SXRD),[14] and ion scattering.[15]

Rutile has also been extensively used in adsorption studies starting from the founding experimental work of Drain and Morrison[16–18] on argon adsorption. Gas adsorption is the most important method for the characterization of mi-croporous and mesoporous materials with regard to surface area and pore size. Adsorption of small molecules or atoms like nitrogen or argon is also a common tool for probing the topography of heterogeneous solid surfaces. From the data obtained from argon adsorption experiments, conclusions about surface topography, namely, surface composition and surface structure can be derived.

In the present work we studied the argon interaction with the (110) crystallographic plane of rutile by density functional theory (DFT) methods. The adsorption of argon on rutile surface is a typical example of a physical adsorption system. As the noble gas has a close-shell electronic structure, the interaction with the surface results from a balance of a van der Waals attraction and Pauli repulsion. This fact poses a challenge to state-of-the-art exchange-correlation functionals, which are believed to not describe properly the dispersion interaction. Nevertheless, at distances near the minima of the adsorption potential, with substantial interaction of the adsorbate and surface orbitals, the short range attraction and the Pauli repulsion are treated appropriately by density functional methods.[19–22] In fact, both local density approximation (LDA) and generalized-gradient approximation (GGA) calculations employing cluster or periodic models provide a correct description of the more attractive sites for adsorption of rare gases on close-packed metal surfaces (see the review of Diehl *et al.*,[23] and references therein). The calculations are in excellent agreement with the most recent experimental results and suggest that, despite the problems associated with DFT functionals, computational data may be used for a better understanding of the physical adsorption of gases on solid substrates.

In further studies we plan to tailor an analytic potential function to reproduce the results of the present calculations,
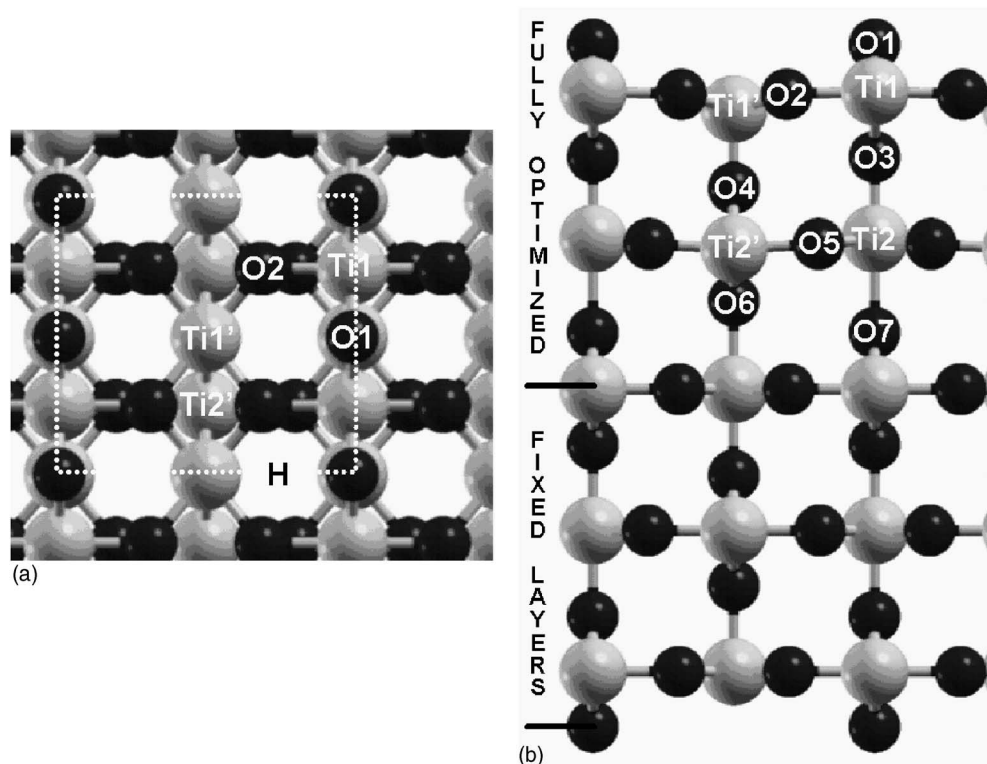
FIG. 1. Top (a) and side (b) views of the 15 atomic layer slab used to model the $TiO_2(110)$ surface. The sites considered for Ar adsorption as well as the 2×1 unit cell used in the calculations are highlighted in (a). The seven fully relaxed atomic layers are shown in (b).

in order to describe the adsorbate-adsorbent interaction in Monte Carlo simulations.

II. METHOD AND TECHNICAL DETAILS

In the present work, the repeated slab periodic approach has been employed to model a perfect clean and infinite $TiO_2(110)$ surface and, also, to represent this surface covered by Ar atoms. Two different slabs were used in the present work and were obtained by truncating the bulk rutile structure perpendicularly to the (110) direction, in such a way that the nonpolar surface is exposed. The nonpolar termination, containing both undercoordinated oxygen and titanium ions, is more stable than the polar ones. This termination is represented in Fig. 1(a) where it is easily noticed the coexistence of surface titanium atoms and two types of surface oxygen atoms (protruding and fully coordinated). A first model was constructed from a 1×1 unit cell with 15 oxygen atomic layers, Fig. 1(b), and used to study the degree of relaxation upon surface cleavage from the perfect bulk TiO_2 rutile structure. A second model based on a 2×2 unit cell with 12 oxygen atomic layers was used to study the interaction between the noble gas atoms and the oxide surface. In the latter situation, the ratio between the number of uniformly deposited Ar atoms and the number of protruding oxygen atoms is $\frac{1}{2}$ and the minimum distance between Ar atoms in adjacent cells is larger than 5.9 Å. This ensures that the contribution of the lateral interactions for the final adsorption states quotient is negligible.

The calculations were carried out using the periodic three-dimensional (3D) VASP code[24–26] and the GGA implementation proposed by Perdew *et al.*[27] The projected augmented-wave (PAW) method due to Blöchl[28] and further implemented by Kresse and Joubert[29] was employed to describe the effect of core electrons on the valence shells together with a plane-wave basis set used to span the valence electronic states. The cutoff energy for the plane waves was 415 eV, and Monkhorst-Pack sets of $8 \times 8 \times 1$ (1×1 cell) or $5 \times 5 \times 1$ (2×1 cell) k points were used. Due to the 3D periodicity imposed by the VASP code, the surface model is in fact repeated in the three dimensions with the slabs being separated by a vacuum width of 10 Å in the z direction. This vacuum width is known to be large enough to prevent layer-to-layer interactions.[5] In order to simulate the bulk environment, some of the slab atomic layers are kept fixed in the calculations, while the outermost upper layers are fully relaxed. During the electronic minimization a blocked Davidson-like algorithm was used and the relaxation of the electronic degrees of freedom stopped when the total free energy and the band structure energy changes were less than 10^{-5} eV. The lattice parameters were set optimized to $a=b$ $=4.634$ Å and the c parameter was chosen in such a way that a vacuum width of 10 Å, in the z direction, was verified between repeated slabs. The parameter u that defines the position of the oxygen atoms on the crystallographic cell, with the Ti atom located at position 0.0; 0.0; 0.0, was optimized to 0.305 fractional units of the crystallographic lattice vectors. All lattice parameters are in excellent agreement with previous GGA-optimized values[30,31] and also with experimental data.[32]
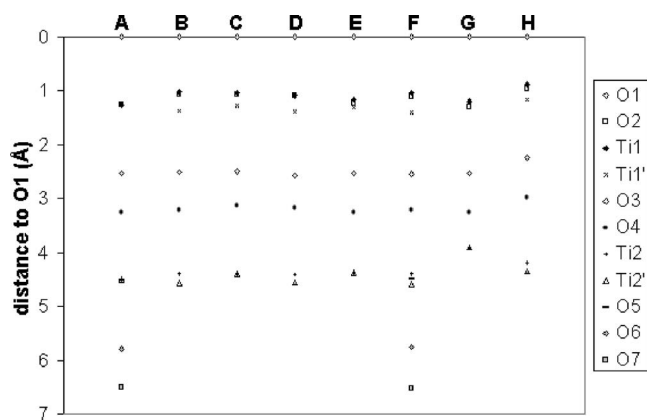
FIG. 2. Comparison between absolute interlayer distances in bulk rutile (A) and computed (B-F) or experimental (G, H) determined interlayer distances of the clean and relaxed $TiO_2(110)$ surface. A—Bulk. B—GGA, 18-layer slab, Ref. 5; C—HF, nine-layer slab Ref. 44; D—LDA, 18-layer slab, Ref. 4; E—LDA, 12-layer slab, Ref. 45; F—GGA, 15-layer slab, this work; G—ICISS, Ref. 46; H—x-ray diffraction, Ref. 47.

Six different sites on rutile (110) surface were considered for Ar adsorption as depicted in Fig. 1(a). For each site, the adsorption energy was calculated as the difference between the energy of the Ar-TiO_2 slab supersystem and the sum of the energies of the free slab and of that of the isolated Ar atom.

III. RESULTS

In order to check the consistency of the present computational approach, the computed surface relaxation is compared with previous theoretical and experimental studies in Fig. 2.

Despite the consideration of a larger slab model and also the full optimization of an increased number of atomic layers, the relaxation of the different atomic layers is in excellent agreement with previous theoretical works. Direct comparison with the work of Bates et al.[5] shows that the 15-layer slab is enough to model the oxide surface and that the full-optimization of inner atomic layers does not change the degree of relaxation of the outermost ions. The maximum deviation in the absolute interatomic relaxations is only 3 pm. In fact, a large number of atomic layers seem to be crucial in the modeling of the rutile surface only if one is interested in deep atomic layer relaxation. This is supported by the identical interatomic distances computed by Reinhardt et al.[44] using a nine-layer model slab and those obtained by the present calculations. The global analysis of the different theoretical methodologies shows that all approaches give similar results with the exception of the LDA/ full-potential linearized augmented plane wave (FLAPW) work of Vogtenhuber et al.[45] The latter approach overestimates the O1-O2 and O1-Ti1 atomic distances and this is probably due to the small number of fully relaxed atomic layers.

The comparison of computed and experimental data shows that a better agreement is found if the Impact-collision ion-scattering spectroscopy (ICISS) results are considered.

However, these experiments do not predict a separation between Ti1 and Ti1′ atomic layers which are suggested by the x-ray experiments and by all theoretical calculations. In fact, separation between Ti2 and Ti2′ layers is also not observed by ICISS. A different and inward relaxation was to be expected for Ti1′ (fivefold coordinated) when compared with the Ti1 ion (sixfold coordinated) due to the loss of coordination of the former ion, in a similar fashion to the large relaxation computed for the outermost Al atoms in α-$Al_2O_3(0001)$.[33,34] The authors do not give any explanation but these surprising results may be caused by difficulties in the measurement of the subsurface electrons during the ICISS experiments.

The adsorption of the Ar atom was considered for six different sites on the relaxed and clean $TiO_2(110)$ surface. The adsorption sites are illustrated in Fig. 1 and are the following: (O1)—Atop outermost oxygen atoms; Ti1—Bridging two outermost O atoms, atop a sixfold coordinated Ti1 atom; Ti1′—Atop fivefold coordinated Ti1′ atom; O2—Atop second-layer oxygen atom; Ti2′—Atop a Ti atom from the forth titanium atomic layer; and H—Hollow site between Ti1 and Ti1′ rows. In an initial stage of our work, the results coming from the optimization of the z coordinate of the Ar atom and from the optimization of the z coordinate of Ar together with the three coordinates of some slab layers were compared. The changes in energy and in the final atomic positions were negligible as expected for this physisorbed system. In fact, some problems with the correct determination of the adsorbate to substrate height were noticed due to the nearly flat energy potential as a function of distance to the surface. Therefore, to avoid some of these problems, the optimization of the Ar atom on the oxide substrate was performed with a frozen substrate. The full set of results (adsorption energies, optimized Ar to surface distances) is presented in Table I while, in Fig. 3, the potential energy as a function of Ar to surface distance is presented.

The calculations show that adsorption above the fivefold coordinated Ti1′ site, in the middle of the protruding oxygen rows, is the most favorable. The calculated interaction energy is 42 meV, which can be compared with experimental data available for Ar adsorption on (111) transition metals (TM) and on MgO(110). The preference for Ti atoms is in agreement with previous experimental findings for the Ar/MgO(100)[35] system where the most stable structures were the ones with a maximum number of Ar atoms occupying Mg sites. In a previous theoretical work employing the GGA/PBE approximation it was predicted an adsorption energy of 76 meV for Xe on Pd(111) and 82 meV on Pt(111).[22] These values are almost 1/3 of the experimentally interaction energies recently determined, ~260 meV for both (111) TM surfaces.[36] In this latter work, Kao et al. have also studied the trapping probabilities of Ar on the Ni group TMs. They predict an interaction energy between 80 and 90 meV for Ar adsorption on Ni(111), Pd(111), and Pt(111). Previously, other authors predicted a similar value, 99±7 meV, for the heat of adsorption of Ar on Ag(111).[37] These values are identical to the suggested heat of adsorption for Ar interacting with the MgO(100) surface.[35] If one considers that the adsorption energies computed with GGA underestimate the energies by a factor of ~3 then one may conclude that the

TABLE I. Adsorption energies, E_{ads} in milli-electron-volts, optimized Ar to nearest-neighbor distances, d(Ar—NN) in angstroms, vertical distance between Ar and O2 atomic layers, d(Ar—O2) in angstroms, and distance between Ar and the nearest-neighbor Ti atom on the surface, d(Ar—Ti$_{NN}$), for Ar adsorbed at the six different sites on the TiO$_2$(110) surface depicted in Fig. 1.

Site	O1	O2	Ti1	Ti1$'$	Ti2$'$	H
E_{ads}	18	28	21	42	33	23
d(Ar—NN)	3.60	4.00	3.89	3.62	3.89	3.60
d(Ar—O2)	4.77	4.00	4.59	3.32	3.70	4.28
d(Ar—Ti$_{NN}$)	4.96	4.46	4.54	3.62	4.28	4.79

strength of the interaction of Ar atoms with the rutile surface is comparable to that of Ar atoms on these TM surfaces. On one hand, this may be used as a validation of the capacity of the GGA/PW91 exchange-correlation functional to provide important data even for a weakly physisorbed state. On the other hand, this may suggest that the weak interaction of rare gases with oxide and metal substrates follows a similar physisorption mechanism.

A general comparison of adsorption on the different sites shows that preference for adsorption on the Ti2$'$ site is only fairly more stable than adsorption on the O2 site. Further, the O1 site is clearly the least preferred. In the recent review of Diehl *et al.*[23] concerning a comparison of the adsorption of rare gases on several surfaces it is suggested that a key element governing noble gas adsorption on close-packed metals is the distance between the adsorbate and the substrate. This is used to explain why rare gases prefer to be adsorbed on top sites (smaller distance to the adsorption site) and not on high-coordination sites as was previously expected for physisorbed atoms. This seems to be the correct picture for rare gas adsorption on all close-packed metals.[23] However, it may change for other substrates as recently found for Xe on graphite where hollow sites are preferred.[38] In the present system, adsorption site preference seems to be also governed by adsorbate to substrate vertical distance, cf., d(Ar—O2) in Table I. However, the interaction of Ar atoms with the rutile

FIG. 3. Calculated adsorption energy of Ar on the six adsorption sites considered for the TiO$_2$(110) surface as a function of distance between Ar and the second-layer oxygen plane.

substrate is not governed by the distance of the rare gas to the nearest neighbor atoms on the surface, cf., d(Ar—NN) in Table I. These findings are somewhat in contrast with the behavior noticed for rare gas adsorption on metallic surfaces. The top position above one Ti atom is the most stable site (Ti1$'$) while the top position above one oxygen atom (O1) is the least stable. Interestingly, for adsorption on the top, but fully coordinated, O2 site the energy of adsorption is higher. In the latter case, the shorter distance to the nearest-neighbor titanium cation may explain the higher adsorption energy. In fact, this seems to be general for the rest of the adsorption positions with the exception of the H site. The calculated interaction preferences for Ar on TiO$_2$(110) are in agreement with previous studies. Preference for adsorption on cationic sites has been reported after high-resolution low-energy electron diffraction experiments on the Ar adsorption above the MgO(100) surface.[35,39] Therefore, a similar adsorption scheme, i.e., directly surface above Ti ions, was to be expected. However, it should be pointed out here that the interaction is somewhat perturbed by the relatively strong inner relaxation of the fivefold coordinated Ti1$'$ ions and to the protruding O1 ions which leave exposed a corrugated surface oxygen layer. Thus, Ar physisorption seems to be both governed by a tendency to move away from anions and to be positioned as close as possible to Ti sites. Thus, adsorption at a Ti—Ti bridge is not to be expected due to the presence of oxygen atoms nearby. These findings are in excellent agreement with previous computational study that points the hybridization of rare gas p orbitals with the unoccupied TM atoms d states near the Fermi level as the primary reason for adsorption site preference.[20]

The interaction between Ar and the TiO$_2$(110) surface is similar to that described previously for Xe adatoms on TM surfaces.[22] In fact, upon approach of Ar to the oxide substrate it is found a broadening of the Ar p states and the appearance of s states. As depicted in Fig. 4, the local density of states (LDOS) for Ar at the optimal distance to the Ti1$'$ site shows a partial occupation of s states. In the present case, occupation of Ar d states was not found as reported previously for Xe adsorption on TM surfaces. This is not surprising due to the larger energetic difference between occupied p and empty d states in Ar when compared with atomic Xe. The reorganization of electronic population is much more evident in the electron density difference—calculated as $\Delta\rho = \rho(\text{Ar}/\text{TiO}_2)\text{-}\rho(\text{Ar})\text{-}\rho(\text{TiO}_2)$—shown in Fig. 5. A strong polarization of the rare gas atom with an electron energy gain in the region between Ar and the Ti1$'$ surface atom and a
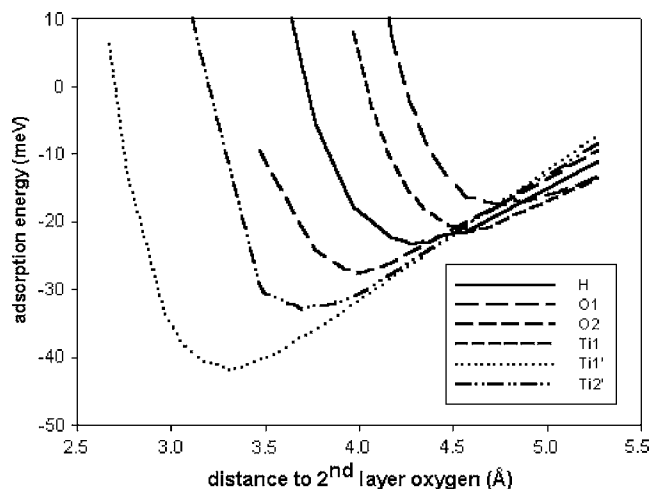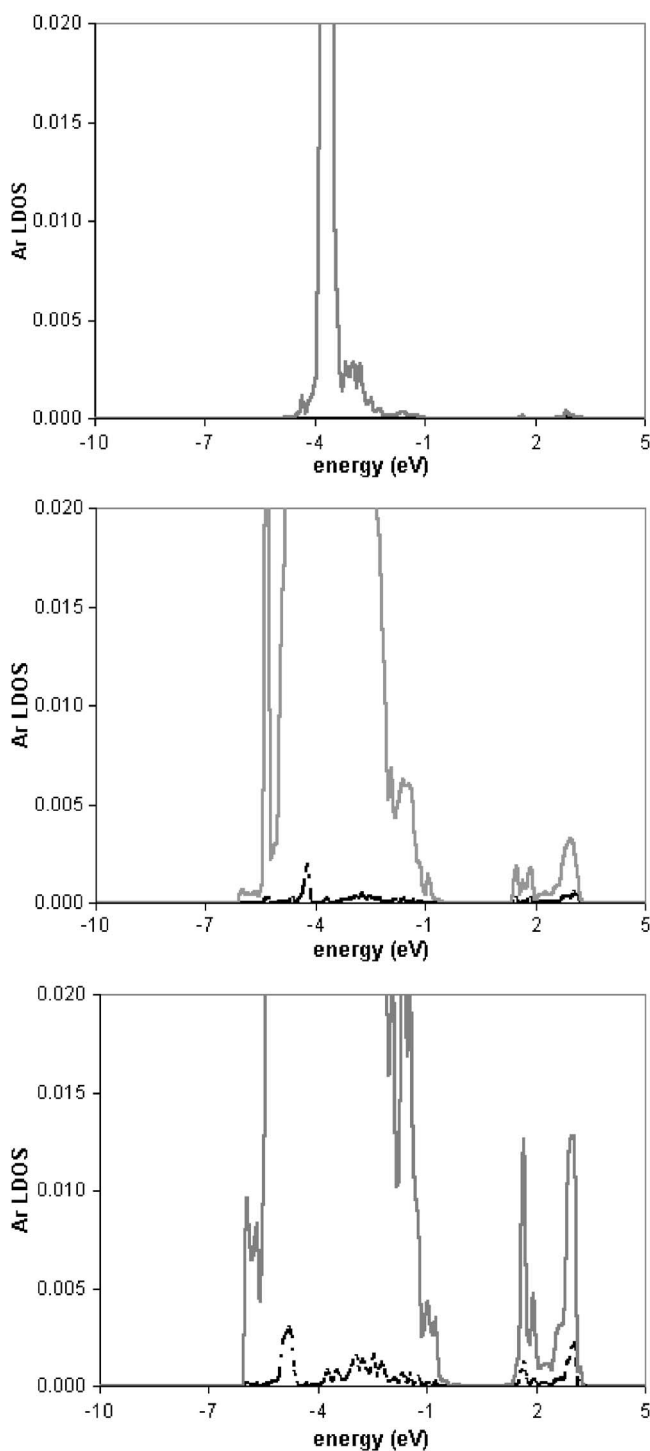
FIG. 4. Local density of states for Ar positioned at three different heights above the Ti1′ site on the TiO$_2$(110) surface. Top: 1.5 Å above the optimized distance; Middle: optimized distance; Bottom: 0.5 Å below the optimized distance. Dotted and solid lines are s and p states, respectively.

FIG. 5. Top (a) and side (b) views of the calculated electron-density differences for Ar adsorbed on the TiO$_2$(110) most stable Ti1′ site. Dark and light gray represent electron density difference isosurfaces corresponding to 1.0 and −1.0 cell volume × electron/Å^3 values, respectively, electron energy gain and electron energy loss with respect to the separated systems.

loss in the region that points to vacuum is found even for a height that is 1.5 Å larger than the optimized value (not shown). For the optimal height, this polarization around the rare-gas atom is enhanced and it is accompanied by some loss of electron density near the Ti1′ site and near the O1
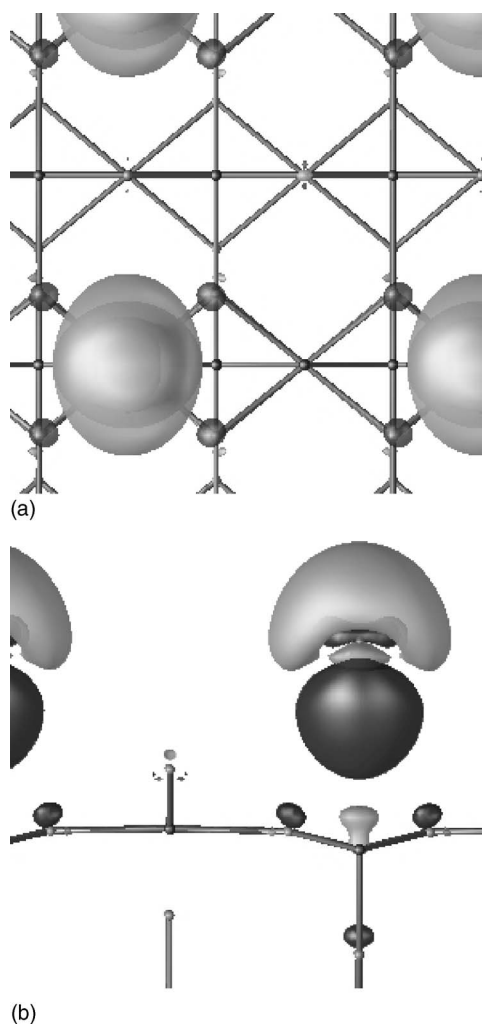
site and a gain of electron density in the oxygen atoms nearby the adsorption site, belonging to the second-oxygen or fourth-oxygen atomic layers. A better understanding of the adsorbate-substrate interaction is obtained from a topological analysis using the Bader approach.[40] A comparison of the Bader charges of the clean and argon covered rutile surface shows a negligible charge transfer from the substrate to the rare gas atom, −0.0014 a.u. A similar finding was previously reported for Xe adsorption on Ag (001)[41,42] although in the latter case a charge of −0.09 a.u. has been transferred. The Bader charge analysis also shows a small charge decrease in the Ti atom (0.0068 a.u.) and a charge increase in the nearby oxygens. This picture is in full agreement with the information retrieved from Fig. 5. The electron localization function (ELF) for Ar located above the Ti1′ site (not shown) presents a perfect spherical core domain on Ar for isosurface values larger than 0.25; for smaller ELF isosurface values, a small distortion is noticed. This bonding scheme resembles

that found for Pd adsorbed above Mg sites on the MgO(001) surface,[43] albeit the interaction is rather more fragile in the case of the rare gas atom. The picture that arises from Figs. 4 and 5 is also similar to that recently given by the theoretical study of Da Silva *et al.* concerning Xe adsorption on metal surfaces.[22] The interaction involves a rearrangement of the charge density both on the rare gas and on the substrate. This rearrangement involves the s and p orbitals of Ar (depopulation of p states and occupation of s states) and a depopulation of metal states and an increase of density in the atomic regions around the adsorption site. This latter effect consisting in the delocalization of charge density, even it seems negligible, diminishes the Pauli repulsion and it permits a better accommodation of the Ar atom on the surface. From that exposed above it may be concluded that the Ar—TiO$_2$(110) adsorption mechanism is dominated by van der Waals interactions. This physisorption description is also supported by the almost identical calculated work functions for the clean TiO$_2$ (110) surface and that for the oxide surface with Ar atoms deposited on the Ti1′ site, $\Phi = 6.90$ eV and $\Phi = 6.85$ eV, respectively. Charge transfer may occur, from the oxide substrate to the adsorbed rare gas atom, but in a negligible extent. This result suggests that, for a larger rare gas atom such as Kr or Xe, the adsorbate-substrate interaction may be important.

As an exploratory study, the full optimization of the three coordinates of two Ar atoms coadsorbed on the same 2×1 unit cell has been carried out. Several different starting geometries have been tested, including that with the rare-gas atoms above the two most stable sites, i.e., one Ar atom above a Ti1′ site and the other above a Ti2′ site. It should be pointed out here that the crystallographic Ar—Ar distance in solid Ar is ~ 3.7 Å and, thus, structures with Ar atoms located in identical adsorption sites on a 2×1 cell are expected to be not stable due to the fact that c parameter of the TiO$_2$ crystallographic cell is ~ 3.0 Å. Therefore, coadsorption of Ar atoms on the two available Ti1′ sites of the 2×1 cell is not stable. The most stable coadsorption configuration is that with one Ar atom above the Ti1′ site while the second Ar atom occupies a Ti1 site, cf. Fig. 6. In this case, the Ar—Ar distance is somewhat larger than that found in solid Ar, 3.99 Å, and the interaction energy is of 23 meV/Ar atom. Two other configurations with adsorption energies per Ar atoms of 18 and 21 meV were also found. The first resembles the optimized geometry depicted in Fig. 6 with one Ar atom close to one Ti1′ site and the other placed between the Ti1 and O2 site and was obtained from a starting geometry with the Ar atoms placed above a Ti1′ and O2 sites. The minimum Ar—Ar distance is now of 3.76 Å. The second configuration was obtained from a starting geometry with the Ar atoms above Ti1′ and hollow sites. During the optimization procedure, the atoms are displaced apart in order to obtain a minimum Ar—Ar distance of 3.94 Å. The final optimized configuration also resembles that reported in Fig. 6. The main difference between these two optimized structures and that shown in Fig. 6 is that when starting with an initial geometry where the Ar atoms are placed in the rows between the protruding oxygen atoms, there is a small energy barrier which prevents the second Ar atom moving atop the Ti1 site, i.e., bridging two protruding oxygen atoms. Since the
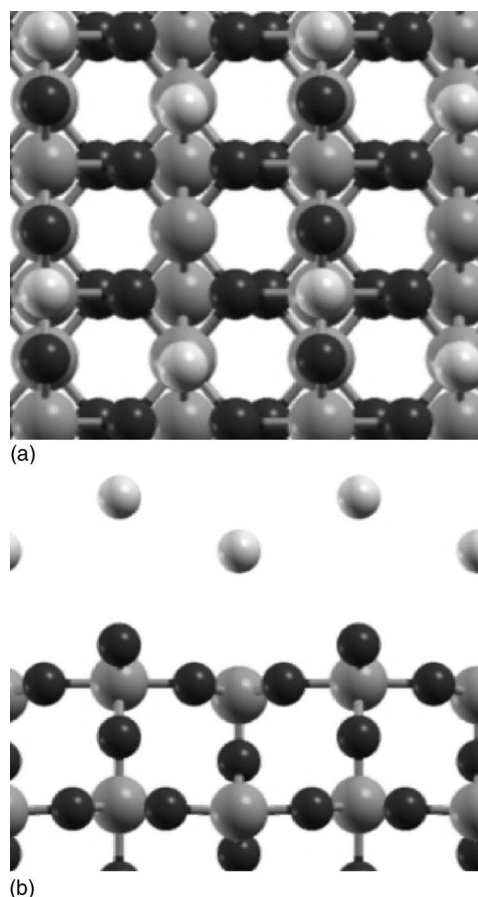

(a)

(b)

FIG. 6. Top (a) and side (b) views of the optimized most stable configuration for two Ar atoms adsorbed on the TiO$_2$(110) surface. The minimum distance between Ar atoms is 3.99 Å.

Ar—Ar distance seems to be the most important parameter determining the final adsorbed configuration, it seems that for an Ar full-covered TiO$_2$(110) surface, structures with Ar atoms positioned above the several different adsorption sites considered in the present work may be expected, in a similar fashion to the mixture of sites suggested for Ar adsorption on MgO(100)[35] and on Ag(111) surfaces.[37]

IV. CONCLUSIONS

The energetics and the geometric structure of Ar atoms on the clean, defect-free and relaxed TiO$_2$(110) surface have been investigated by means of periodic DFT calculations. Six different adsorption sites have been considered, including top, bridge, and hollow positions, involving anions, cations or a mixture of both Ti and O surface atoms. The present calculations show that Ar atoms prefer to be located above the fivefold coordinated titanium atoms and that the less stable sites are above the protruding oxygen atoms. This is in agreement with previous results for the adsorption of rare gases on metal and MgO(100) surfaces. The analysis of the interaction at the Ti1′ sites shows that there is a significant polarization of the adsorbate, with a large dipole mo-

ment pointing towards the surface. This is accompanied by a decrease of charge density near the Ti1′ atom suggesting a decrease in the Pauli repulsion, which permits that the Ar atoms stay closer to the surface in this case than in any of the other five adsorption sites considered. The interaction involves also a redistribution of electronic charge in the Ar atomic orbitals and also a redistribution of electronic charge from the Ti1′ site to the region defined by nearby oxygen atoms.

The coadsorption of Ar atoms on this surface was also analyzed. It is found that the small distance between identical surface sites prevens the coadsorption of two Ar atoms on two Ti1′ sites. Thus, the most stable adsorption configuration is that with one Ar atom above a Ti1′ site and the other above one Ti1 site. However, the calculated adsorption energy per adsorbed Ar atom is only 5 meV larger than that found for Ar atoms on a region above O2 and Ti1 sites. This shows that for larger Ar coverages, the adsorption configuration is not solely determined by the most stable site but also by the Ar—Ar distance that needs to be close to that found in solid Ar matrices.

[1] A. L. Linsevigler, G. Lu, and J. T. Yates, Jr., Chem. Rev. (Washington, D.C.) **95**, 735 (1995).

[2] M. Haruta, Catal. Today **36**, 153 (1997).

[3] K. Pearson, Ind. Minerals **382**, 56 (1999).

[4] M. Ramamoorthy, D. Vanderbilt, and R. King-Smith, Phys. Rev. B **49**, 16721 (1994).

[5] S. Bates, G. Kresse, and M. Gillan, Surf. Sci. **385**, 386 (1997).

[6] J. Muscat, N. M. Harrison, and G. Thornton, Phys. Rev. B **59**, 2320 (1999).

[7] J. Muscat and N. M. Harrison, Surf. Sci. **446**, 119 (2000).

[8] V. Swamy, J. Muscat, J. D. Gale, and N. M. Harrison, Surf. Sci. **504**, 115 (2002).

[9] V. E. Henrich and R. L. Kurtz, Phys. Rev. B **23**, 6280 (1981).

[10] H. Onishi and Y. Iwasawa, Surf. Sci. **313**, L783 (1994).

[11] P. W. Murray, N. G. Condon, and G. Thornton, Phys. Rev. B **51**, 10989 (1995).

[12] U. Diebold, J. F. Anderson, K. O. Ng, and D. Vanderbilt, Phys. Rev. Lett. **77**, 1322 (1996).

[13] R. A. Bennett, P. Stone, N. J. Price, and M. Bowker, Phys. Rev. Lett. **82**, 3831 (1999).

[14] G. Charlton, P. B. Howes, C. L. Nicklin, P. Steadman, J. S. G. Taylor, C. A. Muryn, S. P. Harte, J. Mercer, R. McGrath, D. Norman, T. S. Turner, and G. Thornton, Phys. Rev. Lett. **78**, 495 (1997).

[15] B. Hird and R. A. Armstrong, Surf. Sci. Lett. **385**, L1023 (1997).

[16] J. A. Morrison, J. M. Los, and L. E. Drain, Trans. Faraday Soc. **47**, 1023 (1951).

[17] L. E. Drain and J. A. Morrison, Trans. Faraday Soc. **48**, 316 (1952).

[18] L. E. Drain and J. A. Morrison, Trans. Faraday Soc. **48**, 840 (1952).

[19] N. D. Lang, Phys. Rev. Lett. **46**, 842 (1981).

[20] J. E. Müller, Phys. Rev. Lett. **65**, 3021 (1990).

[21] M. Petersen, S. Wilke, P. Ruggerone, B. Kohler, and M. Scheffler, Phys. Rev. Lett. **76**, 995 (1996).

[22] J. L. F. Da Silva, C. Stampfl, and M. Scheffler, Phys. Rev. Lett. **90**, 066104 (2003).

[23] R. D. Diehl, T. Seyller, M. Caragiu, G. S. Leatherman, N. Ferralis, K. Pussi, P. Kaukasoina, and M. Lindroos, J. Phys.: Condens. Matter **16**, S2839 (2004).

[24] G. Kresse and J. Hafner, Phys. Rev. B **47**, R558 (1993).

[25] G. Kresse and J. Furthmüller, Comput. Mater. Sci. **6**, 15 (1996).

[26] G. Kresse and J. Furthmüller, Phys. Rev. B **54**, 11169 (1996).

[27] J. P. Perdew, J. A. Chevary, S. H. Vosko, K. A. Jackson, M. R. Pederson, D. J. Singh, and C. Fiolhais, Phys. Rev. B **46**, 6671 (1992).

[28] P. E. Blöchl, Phys. Rev. B **50**, 17953 (1994).

[29] G. Kresse and D. Joubert, Phys. Rev. B **59**, 1758 (1999).

[30] N. López and J. K. Norskov, Surf. Sci. **515**, 175 (2002).

[31] Y. Wang and G. S. Hwang, Surf. Sci. **542**, 72 (2003).

[32] U. Diebold, Surf. Sci. Rep. **48**, 53 (2003).

[33] J. R. B. Gomes, I. P. R. Moreira, P. Reinhardt, A. Wander, B. G. Searle, N. M. Harrison, and F. Illas, Chem. Phys. Lett. **341**, 412 (2001).

[34] J. Carrasco, J. R. B. Gomes, and F. Illas, Phys. Rev. B **69**, 064116 (2004).

[35] T. Meichel, J. Suzanne, C. Girard, and C. Girardet, Phys. Rev. B **38**, 3781 (1988).

[36] C.-L. Kao, A. Carlsson, and R. J. Madix, Surf. Sci. **565**, 70 (2004).

[37] J. Unguris, L. W. Bruch, E. R. Moog, and M. B. Webb, Surf. Sci. **109**, 522 (1981).

[38] K. Pussi, J. Smerdon, N. Ferralis, M. Lindroos, R. McGrath, and R. Diehl, Surf. Sci. **548**, 157 (2004).

[39] T. Meichel, J. Suzanne, and J. M. Gay, C. R. Acad. Sci., Ser. II **303**, 989 (1986).

[40] G. Henkelman and A. Arnaldsson, http://theory.cm.utexas.edu/bader/

[41] S. Clarke, G. Bihlmayer, and S. Blügel, Phys. Rev. B **63**, 085416 (2001).

[42] S. Clarke, M. Nekovee, P. K. de Boer, and J. E. Inglesfield, J. Phys.: Condens. Matter **10**, 7777 (1998).

[43] J. R. B. Gomes, F. Illas, and B. Silvi, Chem. Phys. Lett. **388**, 132 (2004).

[44] P. Reinhardt and B. A. Hess, Phys. Rev. B **50**, 12015 (1994).

[45] D. Vogtenhuber, R. Podloucky, A. Neckel, S. G. Steinnemann,

and A. J. Freeman, Phys. Rev. B **49**, 2099 (1994).

[46] E. Asari, T. Suzuki, H. Kawanowa, J. Ahn, W. Hayami, T. Aizawa, and R. Souda, Phys. Rev. B **61**, 5679 (2000).

[47] G. Charlton, P. B. Howes, C. L. Nicklin, P. Steadman, J. S. G. Taylor, C. A. Muryn, S. P. Harte, J. Mercer, R. McGrath, D. Norman, T. S. Turner, and G. Thornton, Phys. Rev. Lett. **78**, 495 (1997).